

Vibronic Coupling in Molecules and in Solids**

Wojciech Grochala,^{*[a]} Roald Hoffmann,^[b] and Peter P. Edwards^[c]

Abstract: We utilize the experience gained in our previous studies on the “chemistry of vibronic coupling” in simple homonuclear and heteronuclear molecules to begin assembling theoretical guidelines for the construction of potentially superconducting solids exhibiting large electron-phonon coupling. For this purpose we analyze similarities between vibronic coupling in isolated molecules and in extended solids. In particular, we study vibronic coupling along the antisymmetric stretch coordinate (Q_{as}) in linear symmetric AAA molecules, and along the optical phonon “pairing” mode coordinate (Q_{opt}) in corresponding one-dimensional $[A]_{\infty}$ chains built of equidistant A atoms. This is done for a broad range of chemical elements (A). The following similarities between vibronic coupling in molecules and phonon coupling in solids emerge

from our calculations: 1) The HOMO/LUMO electronic energy gap in an AAA molecule increases along Q_{as} , and the highest occupied crystal orbital/lowest unoccupied crystal orbital gap in $[A]_{\infty}$ chain increases along Q_{opt} . 2) The maximum vibronic instability is invariably obtained for a half-filled, singly occupied molecular orbital in AAA molecules, and for a corresponding half-filled band in $[A]_{\infty}$ chains. 3) The vibronic stability of an AAA molecule increases with a decrease of the AA bond length, as does the vibronic stability of $[A]_{\infty}$ chains (external pressure may lead to a reversal of a Peierls distortion). 4) The high degree of

s-p mixing and ionic/covalent forbidden curve crossing dramatically enhance the vibronic instability of *both* AAA molecules and $[A]_{\infty}$ chains. We also introduce one quantitative relationship: The parameter $\log(R)$ (where R is molar refractivity, a parameter used by Herzfeld to prescribe the conditions for the metallization of the elements) correlates with a parameter f_{AA} (defined as twice the electronegativity of A, divided by the equilibrium AA bond length), used by two of us previously to describe vibronic coupling in AAA molecules for a broad range of elements (A = halogen, H, or an alkali metal). We hope to illustrate that key chemical aspects of vibronic coupling in simple molecules may thus be profitably transferred to corresponding materials in the solid state.

Keywords: chain structures • conducting materials • solid-state chemistry • superconductors

Introduction

Accepting provisionally the workings of a classical Bardeen–Cooper–Schrieffer (BCS) theory of superconductivity,^[1] one then needs to understand what fundamental science—specif-

ically one might say what “chemistry”—governs the strength of coupling between electrons and optical phonons in extended solids. It could be that a large part of the scientific community has become skeptical during the last decade about the ability of the BCS theory to explain high-temperature superconductivity (HTSC). Yet, it was the very ramifications of the BCS theory which inspired Bednorz and Müller, the discoverers of HTSC, to investigate what are today known as oxocuprates.^[2] Indeed, BCS-related theories of superconductivity still remain a source of inspiration^[3] in the search for a complete understanding of the natural phenomenon of HTSC.^[68]

Unfortunately, “BCS theory” in its original formulation “...lacks material aspect”.^[4] The theory accounts for the phenomenology of the property, but the chemical logic for generating the necessary ingredients for *new* superconductors beyond the oxocuprates is not known.^[5] At present, there is no obvious chemical recipe for HTSC. Our long-term goal is to search for extended systems that might exhibit promising high critical superconducting temperatures (T_c); this is hardly an untypical aim, but what we hope to

[a] Dr. W. Grochala
Department of Chemistry, The University of Warsaw
Pasteur 1, 02093 Warsaw (Poland)
Fax: (+48)22-822-2309
E-mail: wg22@cornell.edu

[b] Prof. R. Hoffmann
Department of Chemistry and Chemical Biology and
Cornell Center for Materials Research
Cornell University, Ithaca NY, 14853-1301 (USA)
Fax: (+1)607-255-5707
E-mail: rh34@cornell.edu

[c] Prof. P. P. Edwards
School of Chemical Sciences, and
Institute of Metallurgy and Materials Science
University of Birmingham, Birmingham, B15 2TT (UK)
Fax: (+44)121-414-4442
E-mail: p.p.edwards@bham.ac.uk

[**] Chemistry of Vibronic Coupling, Part 5; for Part 4 see: ref. [9]

contribute is a chemical perspective coupled with some theoretical guidance.

In previous papers of this series, two of us (W.G. and R.H.) have systematically investigated vibronic coupling in a broad range of simple diatomics and triatomics.^[6, 7, 8, 9] We gathered computational data for hundreds of molecules from the *s*-, *p*-, and *d*-block elements of the Periodic Table with the view of examining systematically key aspects of molecular vibronic coupling. Let us review here the most important general findings of these investigations:

- 1) Molecular systems built of hard Lewis acids/bases are vibronically more unstable than systems built of soft Lewis acids/bases. Strong vibronic coupling should therefore be searched for in molecules built of small, highly electronegative and weakly polarizable atoms;
- 2) The more pronounced the *s*–*p* mixing in molecules, the larger the vibronic instability;
- 3) An “ionic/covalent curve crossing” strongly increases the vibronic instability of a molecule;
- 4) A parameter f_{AB} , defined as the sum of electronegativities of A and B elements, EN_A and EN_B , respectively, divided by the AB equilibrium bond length, R_{AB} :

$$f_{AB} = (EN_A + EN_B)/R_{AB} \quad (1)$$

represents a very useful, quantitative descriptor of vibronic coupling in a molecule. The magnitude of f_{AB} correlates well with the dynamic diagonal coupling constant for ligand-to-metal charge-transfer states of AB diatomics, and also describes off-diagonal vibronic coupling for intervalence charge-transfer states of ABA triatomics.^[10, 11]

In the present contribution, which closes the present series, we analyze different aspects of vibronic coupling in molecules and also in extended systems. We attempt to build the bridge between molecules and solids, to transfer our qualitative and quantitative findings in molecular vibronic coupling to the corresponding situation in the solid state. It is our belief that this might help to design new families of superconducting materials.

Computational Methods and Philosophy

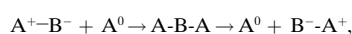
Numerical data have been obtained from density functional theory (DFT) B3LYP computations with 6-31G** or 6-311 + G** basis set for light elements (H, Li, Be, F, Na, and Cl) and LANL2DZ core potentials for heavier elements (K, Rb, Cs, Br, and I). We have used the following computational packages: Gaussian '94^[12] for DFT calculations, YAeH-MOP^[13] and CACAO^[14] for extended Hückel (EH) calculations.

The reader is directed to the four previous parts in this series, where we describe in detail: 1) The nomenclature consistently used by us in these five papers (important, for there is a multitude of terminologies in the field), 2) the basis of simple vibronic coupling models used in the literature, 3) numerical results obtained for a broad range of diatomics and triatomics, and 4) a molecular orbital model used by us to explain vibronic coupling in simple molecules.

We are conscious that local density approximation fails quantitatively (which sometimes leads to qualitative failure— asymmetric and not symmetric structure) for predictions of bond alteration, for example in polyacetylene or radical ions of allene. Yet, it has been adequately demonstrated that even the simplest computational methods, even those which do not contain nonlocal exchange and correlations contributions (such as for example EHT, which exaggerates the strength of vibronic coupling), allow a nice qualitative analysis of the vibronic coupling, rationalization of the origins of the strength of vibronic coupling, and—what is especially valuable— prediction of the trends in the strength of vibronic coupling upon chemical substitution.^[15]

We think that it is desirable to learn from the simplest computational methods, since such methods provide general conclusions at lowest computational cost. They are also physically very transparent, in the sense of allowing one to trace the origins of a trend. In this context, we note that our main goal is not the precise prediction of the absolute tendency of certain molecules (or solids) to distort, but rather the prediction of trends in this tendency in chemically different species and systems. This ranking (relative vibronic coupling strength for different molecules) is far less sensitive to the choice of computational method applied than the absolute vibronic coupling strength.

It needs to be emphasized that the linear symmetric radicals chosen for this study are inherently unstable species. In fact, we have deliberately chosen these species because many of them are highly unstable along the asymmetric stretching vibrational coordinate. The philosophy of our approach, expressed earlier in Parts 3 and 4 in this series,^[8, 9] is to determine quantitatively the instability of such species, and draw general conclusions about the “chemistry of vibronic coupling” for the charge transfer process in the ABA molecule:



which is the simplest system simulating electron transfer between two A centers via an intervening B atom.

The equilibrium geometry of the triatomics (or linear chains) is *not* the concern of the present study—we use these linear geometries as models for tracking down the chemically important effects that determine vibrational instability. The conclusions drawn are quite insensitive to the fact that some of molecular species studied in the Parts 3, 4, and 5 are not relaxed in the full space of nuclear coordinates.

Results and Discussion

Real materials exhibiting superconductivity or strong vibronic (i.e. electron–phonon) coupling will of necessity be complex. However, one of the things we learned in the previous papers is that the underlying physics and chemistry can be explored and modeled with simplified pseudo-hydrogen oligomers (or polymers) in which the component atoms are allowed to vary in electronegativity and other properties. In the next step, *p*

orbitals were modeled, that is we studied a pseudo- E_n (E = main group element, modeled by F) oligomer or polymer.

The paper is organized as follows: In Section 1 we briefly discuss changes in electronic and vibrational structure of H_n species on passing from a linear symmetric H_3 molecule to an infinite chain built of equidistant H atoms. We then analyze vibronic coupling in H_n species along the normal coordinate of a “pairing mode”, passing from isolated molecules to an extended system. In Section 2 we analyze vibronic coupling in a series of A_3^q molecules ($A = \text{Li, H, F, } q = -1, 0, +1$). We then analyze vibronic coupling in the $[H_\infty]^q$ infinite chain, $q \in (-1, +1)$. And we indicate similarities between molecules with a single occupied molecular orbital (SOMO) and an infinite H chain with a half-filled band, in the context of vibronic coupling. In Section 3 we develop an analogy between the dependence of the vibronic stability of heteronuclear ABA molecules on the A–B bondlength, and the dependence of a Peierls distortion in the solid on external pressure. In Section 4 we examine the extreme sensitivity of vibronic stability of both triatomic molecules and solids to the presence of an “avoided crossing” region. In Section 5 we illustrate that the empirical parameter f_{AA} (used by us previously to quantitatively describe vibronic coupling in AAA molecules for $A = \text{halogen, H, alkali metal}$) also correlates well with $\log(R)$, where R is the molar refractivity, a parameter used by Herzfeld in 1927 to describe the metallization of the chemical elements of the periodic classification. In Section 6 we summarize those conclusions on vibronic coupling in simple molecules which may be successfully transferred to the solid state. In the Appendix we discuss briefly the unexpected utility of EH calculations for “pairing mode” force constants.

1. Vibronic stability in $[H]_n$ series—from the H_3 molecule to an infinite hydrogen chain $[H]_\infty$

Assuming the reader is familiar with the evolution of electronic and vibrational structure in the $[H]_n$ series, we will analyze them only briefly; we do need these to interpret vibronic effects further on in this section. Figure 1 illustrates the molecular orbitals (MOs) of the H_3 and H_5 molecules, and selected crystal orbitals (COs) of a 1D $[H]_\infty$ polymer, obtained from the EH calculations.

There are three MOs in the linear symmetric H_3 molecule: the lowermost σ_g (doubly occupied, bonding between each neighboring H atom), σ_u (singly occupied, nonbonding), and σ_g^* (unoccupied, antibonding between each neighboring H atom). There are five MOs in H_5 , seven MOs in H_7 , n MOs in H_n , etc. A simple band structure, a single band (one H atom in

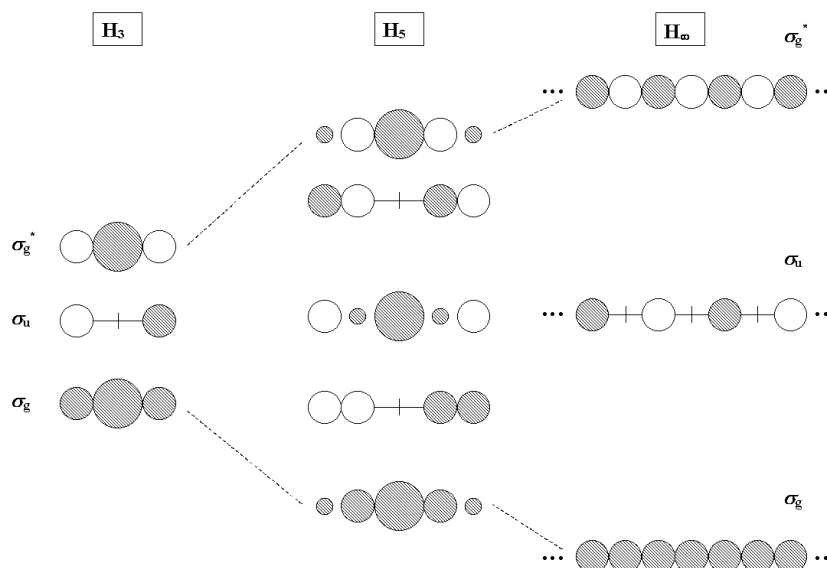


Figure 1. Molecular orbitals of H_3 and H_5 , and three crystal orbitals of a 1D H_∞ polymer (bottom of the band, middle of the band, and the uppermost part of the band).

the unit cell), develops as n increases. The COs of H_∞ may thus be easily derived. The lowermost CO (σ_g), at the bottom of the band, is everywhere bonding. The uppermost CO (σ_g^*) is antibonding between neighboring H atoms, and the (degenerate) CO in the middle between those two is σ_u and nonbonding. These four COs of H_∞ are thus nice analogues of the MOs of H_3 , which epitomizes the nodal structure of any linear molecule.

Let us now examine the evolution of the vibrational spectrum of H_n species as n increases (n is an odd integer). There are three normal modes in a linear symmetric H_3 molecule: symmetric stretching (σ_g), antisymmetric stretching (σ_u), and doubly degenerate bending mode (π_u). In general, there are $(3n - 5)$ vibrational degrees of freedom in a linear H_n molecule: $n - 1$ are reserved for stretching modes (half of these are σ_g , half are σ_u), and the remaining ones belong to the bending modes. From now on we will neglect bending, and concentrate on stretching modes.^[16] Figure 2 shows the evolution of the computed vibrational spectrum of H_n molecules, $n = 3, 5, 7, 9$ (DFT calculations, stretching σ modes only^[17]).

There is one imaginary frequency (a σ_u mode) in the computed vibrational spectrum of the (H_3, H_5, \dots, H_n) series.^[18] There is also a whole family of σ_u and σ_g modes, developing in the real part of the vibrational spectrum as n increases.

Let us look now at the explicit atomic displacements in these normal modes. In Figure 3 we show the forms of the normal vibrations for stretching modes of the H_3 and H_5 molecules, together with familiar form of the “optical phonon” mode of the 1D H_∞ chain.

The imaginary frequency antisymmetric stretching σ_u mode of H_3 is of special interest in our discussions. Apparently it has precisely one counterpart for each $[H]_n$ species. Importantly, each of these imaginary frequency modes, regardless of n , leads to a grouping of H atoms in discrete pairs, leaving one single H aside. These modes also correspond to the optical

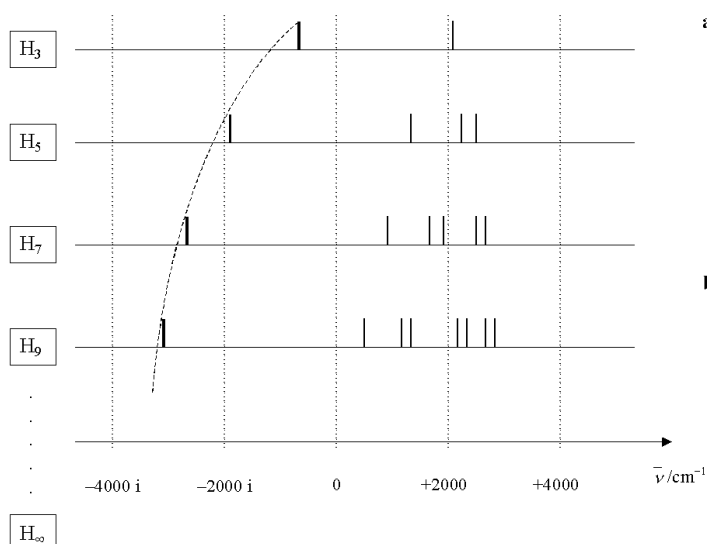


Figure 2. Evolution of the vibrational spectrum in the $[H]_n$ series, $n = 3, 5, 7, 9$ (DFT calculation). Only stretching modes are shown.

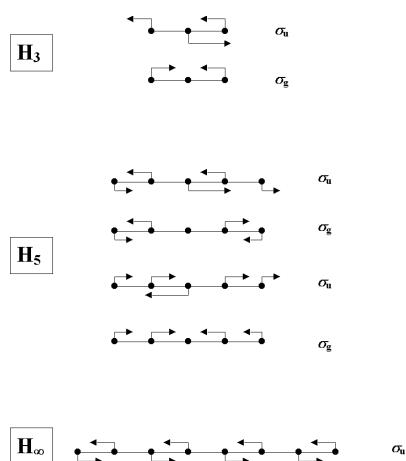


Figure 3. Schematic forms of the normal σ vibrations in the H_3 and H_5 molecules, and the "pairing" phonon σ_u mode of the 1D H_∞ chain. Amplitudes of vibrations are exaggerated.

phonon "pairing" mode of the $[H]_\infty$ infinite chain (Figure 3). The molecular σ_u mode of H_3 is responsible for the vibronic instability of this molecule,^[19] as the phonon σ_u mode is responsible for vibronic instability of the $[H]_\infty$ infinite chain. The latter opens a gap at the Fermi level, and leads to instability of a 1D polymer with a half-filled band, as shown first by Peierls.^[20] Next, we trace in detail an analogy between the influence of molecular and phonon σ_u modes for instability of H_3 molecule and $[H]_\infty$ polymer, respectively.

Figure 4 illustrates schematically the various stages and magnitudes in opening of an electronic energy gap along the Q_{as} coordinate between ground and excited potential energy surface in a linear symmetric A_3 molecule.

Figure 4a and 4b apply to molecules exhibiting a tendency towards spontaneous asymmetrization. Figure 4c and 4d are for molecules which prefer to remain symmetric, while Figure 4a shows a diabatic picture: the gap is zero at $Q_{as} = 0$, and a nonzero energy gap Δ'' opens along Q_{as} . Figure 4b shows an adiabatic representation of the same phenomenon. Now the gap is nonzero at $Q_{as} = 0$ (gap is equal to some Δ'),

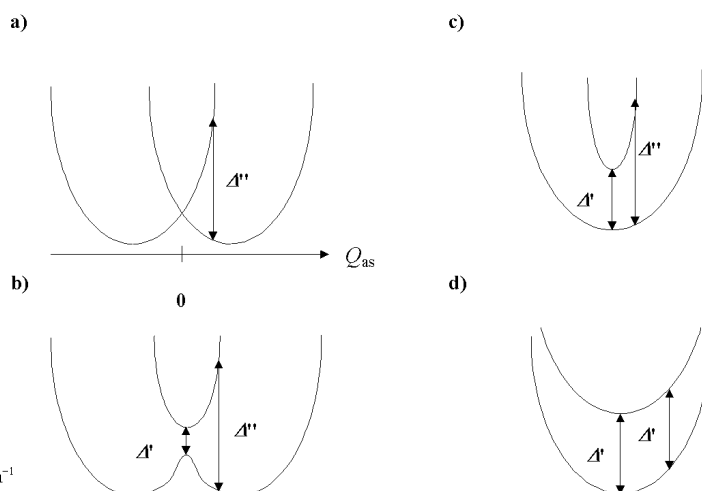


Figure 4. Schematic illustration of vibronic coupling in a molecule: a) Δ' gap opens along Q_{as} between ground and excited state potential energy surfaces in a diabatic model; b) gap increases from Δ' to Δ'' along Q_{as} in an adiabatic model, molecule is asymmetric—case of weak electronic mixing; c) gap increases from Δ' to Δ'' along Q_{as} in an adiabatic model, molecule is symmetric—case of strong electronic mixing; d) gap is constant along Q_{as} —a hypothetical case of zero vibronic coupling. Q_{as} is an ordinate in all cases presented, as shown in (a).

but it increases to Δ'' along Q_{as} . Electronic mixing between lower and higher potential energy surfaces is responsible for the nonzero gap at $Q_{as} = 0$. Figure 4c differs from Figure 4b only in the magnitude of electronic and vibronic coupling. Vibronic coupling is weaker (and/or electronic coupling is stronger) in Figure 4c than in Figure 4b. The linear A_3 molecule now prefers to be symmetric. Yet the energy gap still increases from Δ' to Δ'' along Q_{as} in Figure 4c. A final case might be that of *zero* vibronic coupling. Figure 4d shows such an unrealistic case: the gap is constant along Q_{as} .

As the above examples illustrate, a nonzero vibronic coupling always implies that the energy gap between ground and excited state increases along Q_{as} (regardless of whether a molecule remains symmetric after vibronic coupling, or not). As shown in the previous paper in this series (for example, Figure 9 in reference [9]), an increase of the energy gap between ground and excited is associated mainly with a HOMO/LUMO and a SOMO/LUMO gap increase.^[21]

Changes in the crystal orbital structure (both energies and orbital shapes) of an $[A]_\infty$ 1D polymer due to vibronic coupling are analogous to those of the molecular orbital structure of A_3 molecules (a detailed description of vibronic coupling in H_3 molecule from an MO perspective may be found in our recent paper^[9]). As shown in Figure 5, excursion along the Q_{opt} phonon coordinate leads to opening of the HOCO/LUCO gap. Similarly, excursion along a molecular Q_{as} coordinate in a triatomic molecule leads to an opening of the HOMO/LUMO gap (Figure 4 here, and Figure 9 in reference [9]). These similarities are caused, of course, by analogous topologies of MOs of H_3 and COs of $[H]_\infty$ (see Figure 1).

Let us now describe quantitatively the vibronic stability in the $(H_3, H_5, \dots, H_\infty)$ series. Such a comparison is possible because the reduced mass for all imaginary frequency modes in different H_n species is equal to 1 amu. Figure 6 shows the evolution of the force constants for the imaginary frequency

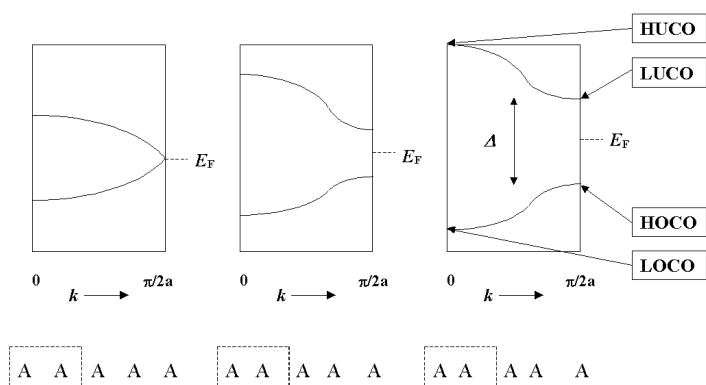


Figure 5. Changes in the band structure of 1D $[A]_{\infty}$ polymer as a function of an excursion along the normal coordinate of optical "pairing" mode Q_{opt} . Q_{opt} is zero on the left (A atoms are equidistant) and increases to the right in the picture. A gap Δ between the highest occupied crystal orbital (HOCO) and lowest unoccupied crystal orbital (LUCO) is zero at $Q_{\text{opt}} = 0$, and increases with Q_{opt} . The energy gap between the highest unoccupied crystal orbital (HUCO) and the lowest occupied crystal orbital (LOCO) also increases with Q_{opt} . The energy of the Fermi level E_F increases from the left to the right in the picture. Dotted lines show the unit cell composed of two A atoms. Diagram is schematic.

σ_u mode in the ($H_3, H_5, \dots, H_{\infty}$) series as a function of the increasing number of H atoms, n .

Figure 6a plots the force constant k_u for the this mode in the ($H_3, H_5, \dots, H_{\infty}$) series; Figure 6b shows the plot of the change in the force constant for the same mode, Δk_u , upon attachment of two H atoms to the H_{n-2} species. Figure 6c presents a plot of the corresponding molar instability (i.e. molar force constant, k_u/n) for the imaginary mode in the ($H_3, H_5, \dots, H_{\infty}$) series as a function of increasing polymer length.

The absolute value of the frequency (or alternatively, the force constant) for the imaginary frequency mode increases with polymer length, as shown in Figure 6a and as emphasized earlier in Figure 2 (see dotted line). However, it may also be seen from Figure 6b that the absolute values of the k_u increments grow smaller with increasing polymer length. The molar stability of the H_n chain passes through a minimum (i.e. maximum instability) for $n = 13$; beyond that it increases slowly with n .

Let us measure the molar instability of the $[H]_{\infty}$ chain by the quantity $(k_u/n)_{\infty}$. The limit may be estimated as $(k_u/n)_{\infty} \approx$

$-0.23 \text{ mDyne } \text{\AA}^{-1}$, extrapolating from the last eight points of the plot presented in Figure 6c (B3LYP/6-31G** calculations). Thus, the 1D $[H]_{\infty}$ polymer built of equidistant H atoms is vibronically unstable, similar to the linear symmetric H_3 molecule ($k_u/3 \approx -0.13 \text{ mDyne } \text{\AA}^{-1}$).^[22]

So far we have traced quantitatively the evolution of the vibronic instability of the $[H]_{\infty}$ polymer, and related it qualitatively to vibronic instability of an H_3 molecule using a simple MO model. An important question, central to all these considerations, comes to mind. Might a ranking of vibronic stability of different A_3 molecules be useful in predicting the vibronic stability of the corresponding $[A]_{\infty}$ 1D chains? For example, does the vibronic stability ranking $Li_3 > I_3 > F_3$ indicate that an analogous electron-phonon coupling ranking $[Li]_{\infty} > [I]_{\infty} > [F]_{\infty}$ would hold? Were this so, many conclusions on vibronic stability of simple triatomics obtained in references [8, 9] might profitably be transferable to a consideration of solid state materials.^[23]

We will not provide an analytic solution to this important problem, but analyze the question semiquantitatively in Section 5.

2. Vibronic coupling in the $(A_3)^0$ linear symmetric radicals (A = Li, F, H) and in the $[A_{\infty}]^0$ 1D infinite chain with a half-filled band

In this section we will concentrate on vibronic coupling in triatomic molecules $(A_3)^q$ as a function of their charge, q . We will also examine the dependence of vibronic stability of the 1D infinite $[A_{\infty}]$ chain on the degree of band filling. In Table 1 we show the optimized bond lengths, R_0 , and force constants for the antisymmetric stretching σ_u mode for a total of nine $(A_3)^q$ species, $A = Li, H, F, q = -1, 0, 1$ (constrained to a linear symmetric geometry^[24]). As may be seen from Table 1, according to our computations, all $(Li_3)^q$ species, H_3^+ and F_3^- are vibronically stable along Q_{as} , (i.e. k_u at R_0 is positive). In contrast, the species H_3, H_3^-, F_3 , and F_3^+ are vibronically unstable, that is k_u at R_0 is negative. Clearly, varying molecular charge (actually changing the occupation of certain MOs) dramatically influences the vibronic stability of $(F_3)^q$ and $(H_3)^q$, but not $(Li_3)^q$ molecules.^[25]

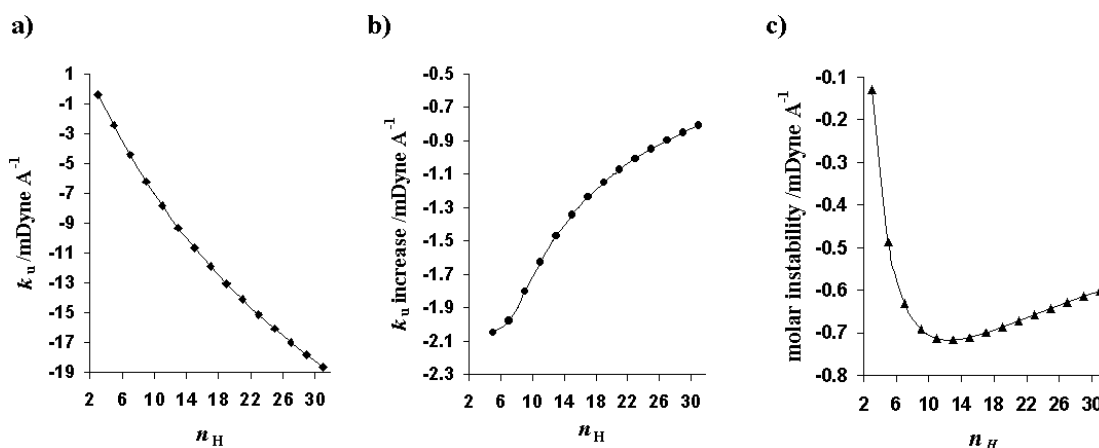


Figure 6. a) k_u , b) k_u increase, and c) molar k_u for the imaginary σ_u mode in H_n species as a function of n . Results of DFT B3LYP/6-31G** calculation.

Table 1. Optimized bond length of linear symmetric $(A_3)^q$ molecules, $A = \text{Li, H, F}$, $q = -1, 0, +1$ (R_0 [\AA]), force constant for the antisymmetric stretching mode determined for the optimized AA bond length (k_u (R_0) [mDynes \AA^{-1}]), and force constant for the antisymmetric stretching mode determined for AA bond length equal to R_0 of $(A_3)^0$ species, $A = \text{Li, H, F}$ (k_u [mDynes \AA^{-1}]). Results of B3LYP/6-31G** calculations.

$(\text{Li}_3)^q$	R_0 [\AA]	k_u (R_0)	k_u (2.885 \AA)
$q = -1$	3.011	0.31	0.43
0	2.885	0.37	0.37
+1	3.001	0.32	0.43
$(\text{H}_3)^q$	R_0 [\AA]	k_u (R_0)	k_u (0.931 \AA)
-1	1.058	-0.90	1.46
0	0.931	-0.32	-0.32
+1	0.820	10.19	4.59
$(\text{F}_3)^q$	R_0 [\AA]	k_u (R_0)	k_u (1.633 \AA)
-1	1.746	2.84	5.35
0	1.633	-35.69	-35.69
+1	1.573	-7.59	-8.48

It is very interesting to compare quantitatively the vibronic stability in the $(A_3)^q$ series. For this purpose we have determined force constants for the antisymmetric stretching modes at a common nuclear separation for $q = -1, 0, 1$. We constrained A–A bond lengths to 0.931 \AA for all $(\text{H}_3)^q$ species, to 1.633 \AA for $(\text{F}_3)^q$ species, and to 2.885 \AA for $(\text{Li}_3)^q$ species.^[26] Numerical data are included in Table 1.

It is clear from Table 1 that there is a *minimum of vibronic stability* (as a function of electron count) in each $(A_3)^q$ series. Interestingly, it occurs for the open shell $(A_3)^0$ species, having a singly occupied molecular orbital (SOMO). For such species, k_u (at certain $R = \text{constant}$), is computed smaller than for the charged closed shell species with one electron more or one electron less. This is true also for $(\text{Li}_3)^0$, although all $(\text{Li}_3)^q$ molecules are vibronically stable. Such an instability of molecular open-shell species is well known. As we show below, this intuitive conclusion is key in designing new solid-state materials with strong vibronic instabilities.

$(A_3)^0$ molecules have an electron count of 1, 1 or 7 electrons per one A atom, for $A = \text{Li, H, and F}$, respectively. Such electron counts would correspond to a half-filled electronic band in 1D infinite $[\text{A}_\infty]$ chains built of these elements. Is vibronic instability in infinite $[\text{A}_\infty]$ chains somehow related to exceptional instability (described above) of molecular open-shell molecules? To answer this question we studied the vibronic stability of 1D infinite $[\text{H}_\infty]$ chains along the “pairing” optical mode as a function of band filling. Figure 7 shows a plot of the frequency of the “pairing” optical mode in the 1D infinite $[\text{H}_\infty]$ chain (ν_u) versus degree of the band filling (EH results).^[27]

As shown in Figure 7, there is a minimum of vibronic stability (as a function of band filling) of the 1D infinite $[\text{H}_\infty]$ chains along the “pairing” optical mode. Maximum susceptibility of polymers to a “pairing” Peierls distortion occurs exactly for a half-filled band. This outcome for the infinite material is not surprising; it has long been known that the driving force for the pairing distortion, the Peierls instability, is strongest for half filling of the H_n band.^[28] Thus, both a linear symmetric triatomic H_3 and a 1D polymer $[\text{H}_\infty]$ are most vibronically unstable for an electron count of $1e^-$ per 1 H

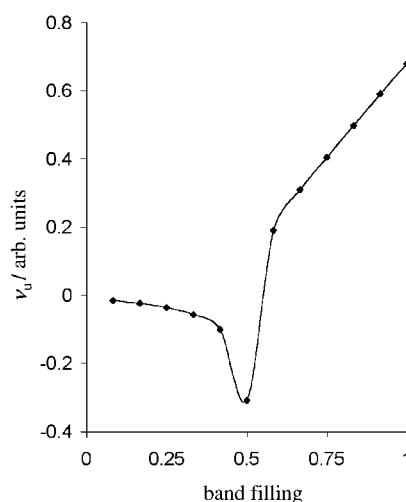


Figure 7. Dependence of the vibronic stability of the $[\text{H}_\infty]$ 1D chain (measured by the frequency of the “pairing” mode, ν_u) on the degree of band filling. EHT results. A negative sign has been arbitrarily introduced for the formally imaginary frequency, for ease of presentation.

atom. This analogy strongly points to the underlying similarity of vibronic effects in molecules and in the corresponding extended solids.

3. Peierls distortion in 1D solids as a function of external pressure, and vibronic coupling in linear symmetric ABA^0 radicals as a function of the A–B bond length

In this section we will investigate further analogies between vibronic coupling in molecules and in solids. We concentrate on the dependence of vibronic coupling in linear symmetric ABA^0 radicals on the A–B bond length, and on the Peierls instability in 1D solids as a function of the external pressure. We will start our considerations from triatomics. Figure 8 shows the computed force constant for the antisymmetric stretching mode, k_u , in three linear symmetric ABA molecules, H_3 , Be_2I , and Na_2F , as a function of the A–B bond length, R_0 . As shown in Figure 8, the vibronic stability of an H_3 molecule depends strongly on the H–H bond length. In principle, k_u is a monotonic and decreasing function of the

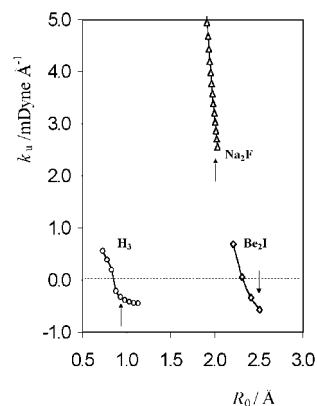


Figure 8. Dependence of force constants for antisymmetric stretching σ_u modes on the A–B bond lengths in linear symmetric ABA molecules. a) H_3 , b) Be_2I , c) Na_2F . Arrows indicate the equilibrium A–B bond lengths. DFT/6-311 + G** calculations.

H–H bond length.^[29] The H_3 molecule with $R_0 = 0.931 \text{ \AA}$ (lowest energy with a $D_{\infty h}$ constraint) is vibronically unstable. Elongation/shortening of the H–H bond length respectively increases/decreases the susceptibility of H_3 towards asymmetrization, as measured by k_u . H_3 becomes vibronically stable for $R_0 < \text{about } 0.85 \text{ \AA}$ (k_u is positive). Similar k_u versus R_0 dependences (as far as trends are concerned) are computed for Be_2I and Na_2F (Figure 8), and seen in Table 1 for $(A_3)^q$ molecules ($A = Li, H, F, q = -1, +1$). In all cases k_u is a monotonic and decreasing function of the A–B bondlength.

The reversal of a Peierls instability by applying external pressure, a phenomenon very similar to what the above computations point to, is well-known for 1D solids.^[30] Figure 9

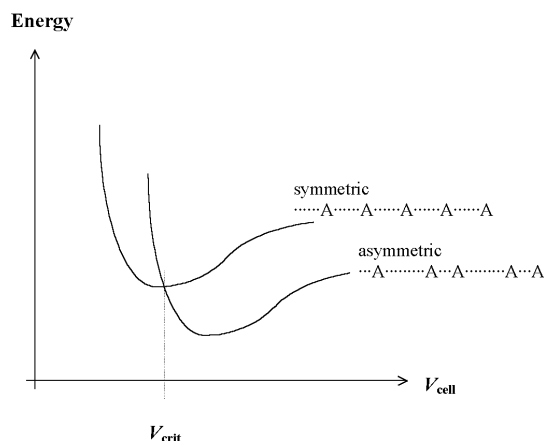


Figure 9. Dependence of the energy of Peierls undistorted (symmetric) and Peierls distorted (asymmetric) 1D $[A]_{\infty}$ chain on the volume of the unit cell V_{cell} . The Peierls distorted structure has global energy lower than the symmetric one, and the symmetric structure spontaneously distorts along the “pairing” mode normal coordinate. Increase of external pressure decreases the unit cell volume, and leads to inversion of the Peierls distortion below a certain critical value of V_{cell} , $V_{\text{cell}} < V_{\text{crit}}$.

shows the dependence of the energy of Peierls undistorted (symmetric) and Peierls distorted (asymmetric) 1D $[A]_{\infty}$ chain on the volume (length) of the unit cell V_{cell} . Note that the Peierls-distorted (asymmetric) structure has its global energy minimum lower than the symmetric one, and the symmetric structure spontaneously distorts along the “pairing” mode normal coordinate (above a certain unit cell volume). An increase of external pressure decreases the unit cell volume, and leads to a reversal of the Peierls distortion below a certain critical value of V_{cell} , for $V_{\text{cell}} < V_{\text{crit}}$.

Thus, there is another analogy between simple linear symmetric triatomics and 1D solids, now in the context of the pressure dependence of vibronic coupling.

4. Influence of s–p mixing and “avoided crossing” on vibronic coupling in molecules and in solids

We have recently analyzed in detail the strong influence of s–p mixing and “avoided crossing” on vibronic coupling in simple triatomics.^[9] We have shown that increased s–p mixing, especially in the vicinity of the avoided crossing region, dramatically increases the vibronic instability of the model F_3 molecule. Since avoided crossing of potential energy surfaces seems to be an important factor influencing vibronic coupling in molecules, we wish to analyze its role in vibronic coupling in solids.

How to study s–p mixing? The extended Hückel method allows one to do this by varying the energies (the H_{ii} parameters of the theory), while keeping the atomic exponents fixed. Using this procedure, we computed the dependence of a) the force constant for the antisymmetric stretching mode in the F_3 molecule and b) the force constant for the “pairing” optical phonon mode in a 1D $[F]_{\infty}$ chain built of equidistant F atoms, on the difference between extended Hückel H_{ii} for 2s and 2p orbitals of F atom, ΔH_{ii} (s–p). The H_{ii} 's for 2s orbital of a) the central F atom in the F_3 molecule, and b) each second F atom in the 1D $[F]_{\infty}$ chain have been varied, respectively. Figure 10 shows the results of the EH computations. Clearly, s–p mixing influences strongly the vibronic stability of both the F_3 molecule and the 1D $[F]_{\infty}$ chain. There is a region of strong instability (minimum of k_u), around ΔH_{ii} (s–p) = 2 eV, for both F_3 and $[F]_{\infty}$. It corresponds to a (physically unrealistic) “2s over 2p” orbital ordering in the vicinity of the “avoided crossing” region.^[31] The region of the strong vibronic instability is narrower (on the ΔH_{ii} (s–p) scale), and the k_u versus the ΔH_{ii} (s–p) dependence is steeper (especially on the right side of the minimum) for $[F]_{\infty}$ than for F_3 . The cross-over region is unrealistic, but the trend is important, pointing to analogous behavior in the molecule and the one-dimensional solid.

As shown in this section, there is a strong analogy between simple linear symmetric triatomics and 1D solids in the

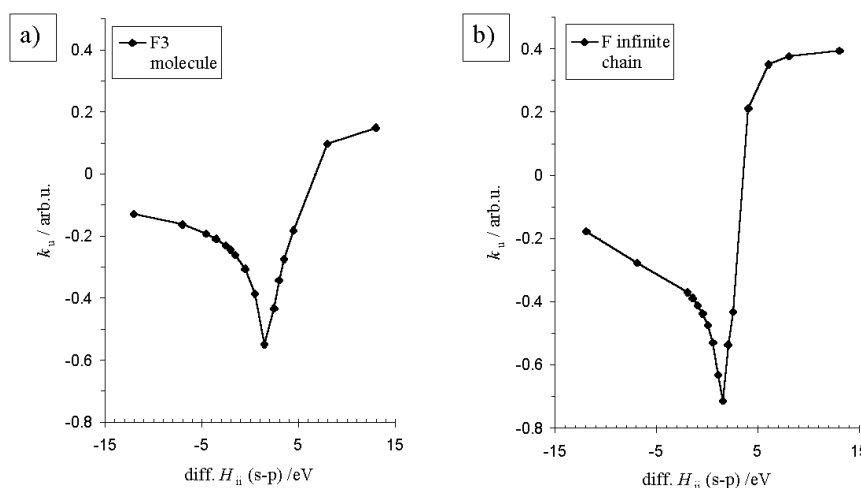


Figure 10. Dependence of a) the force constant for the antisymmetric stretching mode in the F_3 molecule and b) the force constant for the “pairing” optical phonon mode in 1D $[F]_{\infty}$ chain built of equidistant F atoms, on the difference between extended Hückel H_{ii} for 2s and 2p orbitals of F atom, $\text{diff. } H_{ii}$ (s–p). The H_{ii} 's for 2s orbital of a) central F atom in the F_3 molecule, and b) of each second F atom in the 1D $[F]_{\infty}$ chain, respectively, have been varied.

context of coupling of electrons with vibrations of nuclei. This analogy extends to the strong influence of s–p mixing and of the “avoided crossing” region on vibronic instability.^[32] These results suggest that inorganic chemists should search carefully for solid state systems exhibiting “avoided crossing” regimes, for example such as Equation (2a) or (2b) and utilize them in the synthesis of new materials potentially exhibiting strong vibronic coupling.



The process described by Equation (2a) has indeed been suggested previously as being crucial for high-temperature superconductivity in oxocuprate materials.^[33]

5. The metallization of the chemical elements and vibronic coupling in molecules

The Peierls distortion, and more generally the phenomenon of vibronic coupling in solids, is intimately connected to the long-standing problem of the metallization of insulators.^[34] For example, in the simplest 1D case, a Peierls distortion of a metallic chain of equidistant H atoms leads to appearance of insulating behavior in a polymer that transforms to a chain built of H₂ molecules. Also for “real” 3D solids, the reversal of a Peierls distortion (say, under pressure) may lead to metallization of a sample.^[35]

Experiment shows that usually the more electronegative element A, the larger the vibronic instability in the metallic phase of A, and hence the larger the external pressure needed to metallize A. So far, even the strongly electronegative elements (colloquially called “nonmetals”), such as Xe,^[36] O,^[37] Br,^[38] I,^[39] and S^[40] have been metallized by application of very high pressures. Many “ionic” insulators such as CsI^[41, 42] or BaSe^[43] have also been metallized. As far as we know, only H^[44] (solid), N, Cl, F, and four noble gases (He–Kr) have not been metallized so far among the chemical elements of the Periodic Table.

The Peierls distortion (leading to insulating behavior of what might have been a metal) is connected with the opening or appearance of an electronic band gap at the Fermi level. Superconductivity is also connected with the dynamic opening of a (superconducting) band gap near the Fermi level,^[45] as predicted by BCS theory.^[1] And, interestingly, superconductivity appears in many materials previously metallized by applying external pressure, such as metallic S,^[46] O,^[47] B,^[48] I,^[49] SnI₄,^[50] SnSe^[51] and CsI^[42]. There are even suggestions that Xe might be superconducting under high pressures.^[52] In addition, substances that are superconducting at ambient conditions, are usually strongly sensitive to external pressure.^[53] No surprise, then, that there have been many interesting attempts to interrelate superconductivity with susceptibilities, or proximity of chemical compounds to the pressure-induced insulator-to-metal transition.^[54] Let us mention the efforts of Burdett and coworkers to simultaneously describe metallic character^[55] and superconductivity^[33] through a *dynamic band gap opening*, which will be of a special interest to us. We believe that Burdett’s viewpoint is

important and may be potentially be translated into chemical language; it may, in perspective, also stimulate the design of new superconducting materials.

Given the implied strong relationship between the tendency toward—and competition between—metallization and superconductivity, let us investigate now the former phenomena from a distinctly chemical viewpoint, that of the polarization, or dielectric catastrophe accompanying the metallization of elements and materials.

The first semiquantitative attempts to explain the occurrence of metallic behavior in the periodic system of the elements, and other systems, were made by Goldhammer^[56] in 1913 and Herzfeld in 1927.^[57] The Goldhammer–Herzfeld approach is concerned with the mutual polarization of an atom or molecule by the remaining particles in the condensed phase (be it liquid or solid). A straightforward illustration of Herzfeld’s approach can be made by considering a simple classical atom in which a point positive charge is surrounded by a spherically-symmetric negatively charged cloud of constant density, extending out to some characteristic radius r . This is equivalent to the model of the atom as a perfect conducting sphere. From electrostatics, it can be shown that the electronic polarizability, α_0 , of such a species is given by Equation (3).

$$\alpha_0 = r^3 \quad (3)$$

Its associated molar refractivity, R , is then given by Equation (4), where N_A is the Avogadro number.

$$R = \frac{4}{3}\pi N_A \alpha_0 \quad (4)$$

Now R/N_A is thus a measure of the volume of the isolated atom. We now place such an atom in a Lorentz cavity in a dielectric medium. Within the condensed phase, the molar volume, V , represents the portion of space associated with a given particle (atom). In this model, metallization occurs when the available volume in the condensed phase becomes equal to, or less than, R ; under these conditions the system of localized perfectly conducting spheres then gives way to one large, macroscopic conductor, across the entire volume of the material. We then have a transition to the metallic state at some critical molar volume for a given value of R .

Herzfeld proposed what is now known as a polarization or dielectric catastrophe at metallization, and the idea that the dielectric constant, ϵ , of the condensed phase should diverge to infinity as an insulator-to-metal transition is approached from the insulating side. This means that the dispersion (valence) electrons, which before had been quasielastically bound, classically speaking, to their own atoms or ions, are now set free through mutual interactions in the condensed phase, and the system becomes a metallic conductor.

The ideas are perhaps most easily cast in terms of the Clausius–Mossotti relation [Eq. (5)], where ϵ is the high-frequency dielectric constant and n is the optical refractive index;

$$(\epsilon - 1)/(\epsilon + 2) = (n^2 - 1)/(n^2 + 2) = R/V \quad (5)$$

Thus, the Herzfeld metallization criterion [Eq. (6)] specifies a situation in which ε (equivalently n^2) must equal infinity.^[58]

$$R/V=1 \quad (6)$$

The simple Herzfeld model is in remarkably good agreement with considerably more complex theoretical predictions for the conditions necessary for the metallization of the chemical elements, and many other systems.^[59] What values does the Herzfeld parameter (R/V) take in the Periodic Table of elements under ambient conditions? Figure 11 shows $\log(R/V)$ for different elements, as given in contributions of Edwards and co-workers.^[59]

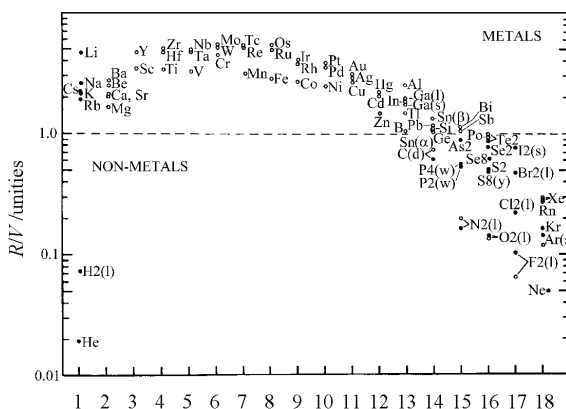


Figure 11. Plot of Herzfeld's parameter R/V used to describe metallization of elements. Dotted line separates metals from nonmetals.^[59a]

The characteristic parameter (R/V) takes on the smallest values for the most electronegative elements, such as F, Cl, O, the noble gases, and H. These elements are now known to be the most difficult to metallize under pressure. The empirical borderline between metallic and insulating behavior lies at $\log(R/V) = 1$. The strongest vibronic instability (measured by negative force constant) has been calculated by us for F_3 , Cl_2F , and H_2F among simple triatomics.^[8,9] Could the experimental observations of propensity (or lack of it) toward metallization for extended systems be somehow correlated with our findings on vibronic coupling of simple molecules^[60]? Let us make an attempt at such a correlation.

We have recently introduced an empirical parameter f_{AB} , defined as the sum of Pauling electronegativities of the A and B elements, divided by the A–B bond length and we have successfully used f_{AB} to correlate, semiquantitatively, the strength of vibronic coupling in diatomics and triatomics.

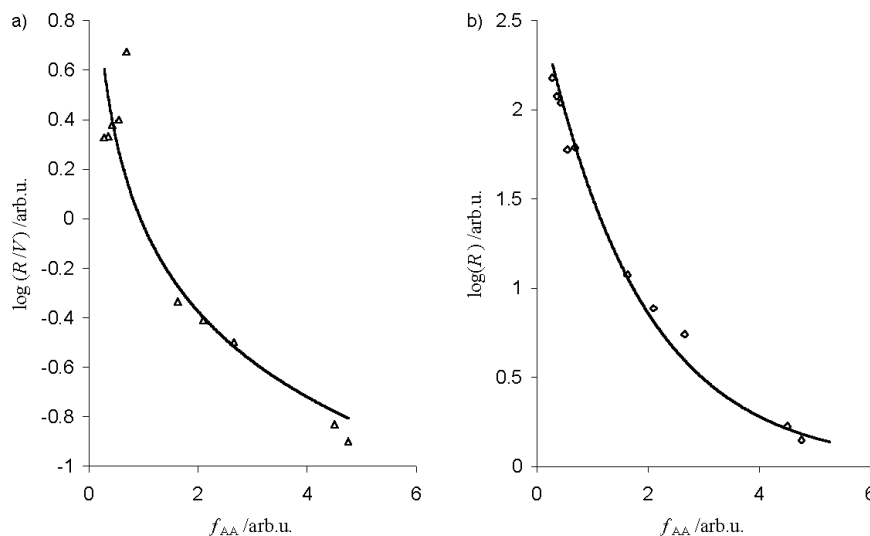


Figure 12. Correlations between $\log(R/V)$ and f_{AA} , and between $\log(R)$ and f_{AA} , where R/V is Herzfeld's parameter used to describe metallization of elements, and f_{AA} is defined as twice the electronegativity of element A divided by the AA bond length. A = F, Cl, Br, I, H, Li, Na, K, Rb, Cs. Fits to exponential regressions are shown by solid lines.

Let us try now to correlate f_{AA} (as determined for simple AAA triatomics) with the metallization tendency of element A, as described by Herzfeld's parameter (R/V) for standard conditions of density, etc.

We have chosen 10 different chemical elements to attempt this correlation: four halogens (F, Cl, Br, I), hydrogen (H), and five alkali metals (Li, Na, K, Rb, Cs). These elements enter in diatomic homonuclear molecules as monovalent species; they usually occur in chemical compounds as anions (halogens) and as cations (alkali metals). These various families were chosen since they undoubtedly represent the extremes of chemical properties, from the most electronegative—gaseous, oxidizing fluorine—to the most electropositive, metallic cesium. Such a choice naturally provides a large range for us to compare R , (R/V), and f_{AA} parameters.

The resulting correlations between $\log(R/V)$ and f_{AA} , and between $\log(R)$ and f_{AA} for these 10 elements are shown in Figure 12a and 12b. It appears from Figure 12 that there is an excellent correlation between f_{AA} and $\log(R)$. A correlation factor of $r^2 = 0.988$ has been found for exponential regression. Correlation of f_{AA} with $\log(R/V)$ is somewhat worse ($r^2 = 0.863$). It appears that a further evaluation of the Herzfeld criterion, paying particular attention to the correlation of R with f_{AA} , is now called for.

Searching for the qualitative explanation of the monotonic relationship between f_{AA} and $\log(R)$, we have tested additional correlations of $\log(R)$ with f_{AA} . We have tried defining f_{AA} according to the Equation (1), using however the Mulliken electronegativity^[61] instead of the Pauling one. This correlation yielded a somewhat worse correlation factor of $r^2 = 0.986$. Alternatively, we have used the absolute hardness^[61] ($r^2 = 0.952$) or configuration energy^[62] ($r^2 = 0.993$) instead of Pauling electronegativity entering the formula in Equation (1).

The quality of all the above correlations is surprisingly good. It means that the susceptibility of an A_3 molecule to vibronic coupling appears to be strongly related to the

characteristic molar refractivity, R , of the element A (recollect that the latter is proportional to the electronic polarizability of A, [Eq. (4)]). A useful way of thinking of electronic polarizability is that it represents the ease with which electronic excited states can be mixed into the ground state to induce charge polarity. Furthermore it can be demonstrated that the mean dipole moment of an atom goes to infinity as the dielectric catastrophe is approached.^[59c] This is equivalent to saying that the onset of itinerancy (metallization) in the condensed phase is manifest in a mechanical instability of the harmonically bound electron to its parent nucleus. Similarly, the more pronounced the s–p mixing, the larger is the polarizability of the A_3 molecule, and the larger its vibronic instability. These simple physical arguments may be at the heart of these strong correlations (Figure 12). We are currently exploring further the quantitative features behind the excellent quality of the correlation between f_{AA} and $\log(R)$ across so many different elements.

Suffice it to say that the correlations observed between f_{AA} and $\log(R)$ and between f_{AA} and $\log(R/V)$ for a great variety of chemical elements show that studies on vibronic coupling in simple molecular systems may be very useful in predicting metallization and, perhaps, ultimately the appearance of superconductivity in materials. Recollect that it is sulfur, a nonmetal, which surprisingly holds the present record of T_C among the elementary superconductors (under high pressure).^[46] Who knows, maybe metallic fluorine—if ever obtainable—will surprise us even more.

6. Which phenomena and conclusions related to vibronic coupling may therefore be transferred from molecules to solids?

Let us summarize the most important conclusions from the previous sections. The following analogies between vibronic coupling in pseudo- H_3 molecules and in 1D pseudo- $[H]_\infty$ solids are found:

- 1) The analogous electronic structures of H_3 molecules and 1D $[H]_\infty$ chains imply similar consequences for vibronic mixing of molecular/crystal orbitals along the antisymmetric stretching/“pairing optical phonon mode” or Peierls distortion σ_u coordinate, respectively. The HO-MO/LUMO gap increases in H_3 molecules along σ_u coordinate,^[21] as does the LOCO/HUCO gap in $[H]_\infty$ chains with pairing.
- 2) A parallel dependence of vibronic stability of A_3 molecules and of $[A]_\infty$ polymers on the degree of band filling, is another remarkable similarity between molecules and solids. Both A_3 molecules and $[A]_\infty$ solids exhibit the most pronounced vibronic instability for the same electron count of $1e^-$ /atom for $A = H, Li$, and of $7e^-$ /atom for $A = F$. This corresponds to open-shell A_3 molecules, and to $[A]_\infty$ solids with a half-filled band.
- 3) A dependence of the vibronic stability of A_3 molecules on the A–A bond length is another feature of molecular vibronic coupling closely related to phonon coupling in solids. Linear symmetric A_3 molecules become vibronically more stable with decreasing AA bond length. This is similar to the well-established Peierls distortion in 1D

$[A]_\infty$ solids, which may be reversed or prevented from happening by applying external pressure.

- 4) Vibronic mixing in A_3 molecules and $[A]_\infty$ solids exhibits similar sensitivity to the s–p mixing, and to the “avoided crossing” of electronic levels. Vibronic instability of both the A_3 molecules and the $[A]_\infty$ solids increases strongly with enhanced s–p mixing, especially in the vicinity of an avoided crossing. The presence of the avoided crossing region is crucial for strong vibronic coupling. This feature may be of pivotal use for the deliberate design of molecules and solids exhibiting strong vibronic coupling.
- 5) An important quantitative relationship has been found connecting molecules and solids in the context of vibronic instability. The semiempirical parameter f_{AA} defined as twice the electronegativity of element A, divided by the A–A bond length in the AAA molecule, correlates extremely well with $\log(R)$, where R is molar refractivity, a parameter used by Herzfeld to describe the metallization of the chemical elements. This correlation has been found for elements with markedly different chemical and physical properties, $A = F, Cl, Br, I, H, Li, Na, K, Rb, Cs$, ranging from the most electronegative to the most electropositive elements within the periodic classification.

In this paper we have considered only 1D solids. However, we have also investigated the vibronic stability of 1D, 2D, and 3D structures built of H atoms (unpublished B3LYP/6-31G** results). For this purpose we computed force constants for the imaginary modes with the largest absolute value of frequency for linear H_3 , a square symmetry H_9 , and cubic H_{27} . We find that vibronic stability and molar vibronic stability strongly decrease in the order H_3, H_9, H_{27} , that is with the increasing dimensionality of the *finite* structure. These results point to strong nonadditivity of vibronic effects. Substantial cooperativity of vibronic effects is expected for high-symmetry *infinite* H nets, as well. We expect molar vibronic stability to decrease strongly as one constructs a 3D infinite cubic crystal by bringing together 2D planes, which have been obtained from 1D $[H]_\infty$ chains gradually approaching one another. Or in general for strongly connected 3D networks.

Conclusion

One is often led to thinking of molecules and of extended solids as two separate worlds. There are few compelling reasons to think so.^[63, 64]

We have devoted four previous contributions in this series to the “chemistry of vibronic coupling” in simple molecules. In these papers we have shown how to design molecules exhibiting strong vibronic coupling. In the present contribution we have performed analyses of both similarities and differences between molecules and extended systems in the context of electron-vibration (vibronic) coupling. We have demonstrated many parallels in vibronic coupling in A_3 molecules and $[A]_\infty$ solids. Many conclusions on the “chemistry of vibronic coupling” in molecules may thus be transferred to solid state materials. Our findings, combined with important ingredients originating from works of Sleight^[65] and Johnson,^[3] might help to design solids with strong electron-

phonon coupling, and, possibly, novel families of superconductors.

Indeed, the findings presented in this series of five theoretical papers led us to a specific theoretical search for superconductivity in the complex fluorides. The anion F^- is the hardest, the least polarizable and the most difficultly oxidizable anion available in chemistry. Searching for ways to approach the forbidden (neutral/ionic) crossing in fluoride materials (thus, the quest for a “polarizable fluoride ion”), we were forced to look to inorganic chemistry at its very limits of positive redox potentials. Thus, we have predicted elsewhere that superconductivity may exist in hole-doped fluorides of Ag^I , fascinating and relatively unexplored inorganic materials.^[66] Experimental evidence for superconductivity in these fluoroargentates is now actively being sought in several laboratories.

Acknowledgement

This research was conducted using the resources of the Cornell Theory Center, which receives funding from Cornell University, New York State, the National Center for Research Resources at the National Institutes of Health, the National Science Foundation, the Defense Department Modernization Program, the United States Department of Agriculture, and corporate partners. This work was supported by the Cornell Center for Materials Research (CCMR), a Materials Research Science and Engineering Center of the National Science Foundation (DMR-9632275) and by NSF Research Grant (CHE 99-70089). We also acknowledge the Royal Society (UK) for support. The Referees are acknowledged for their constructive criticism, which helped us to improve our initial manuscript.

Appendix

Unexpected utility of EH calculations in estimating the force constant for the imaginary “pairing” mode in linear H_n molecules

Several results in this paper originate from the EH calculations (those presented in Figures 7 and 10). The EH theory generally produces highly unsatisfactory vibrational spectra. We would like to discuss now an unexpected range of validity of EH calculations of force constants for the antisymmetric stretching mode in linear symmetric A_3 molecules and for the imaginary frequency optical phonon mode in $[A]_\infty$ solids built of equidistant chain of A atoms.

We have computed vibrational spectra of linear H_3 , H_5 , H_7 and H_9 molecules using EH and DFT (B3LYP/6-311++G**). Vibrational spectra have also been computed by EH using normal coordinates determined in DFT calculations. The EHT computations indeed give vibrational spectra that are on an absolute scale way off the (presumably better) DFT values. Then we tried to correlate the imaginary frequency modes^[67] of as computed by DFT and EH. This correlation is presented in Figure 13. As may be seen in Figure 13, the vibrational frequency for the imaginary mode computed by EH correlates very well with one obtained from DFT calculations. The correlation factor is $r^2 = 0.996$. Of course, EH does not predict properly the absolute values of these imaginary frequencies, nor absolute vibronic stability: the linear regression presented in Figure 13 does not cross the origin. However, clearly one may trust the *trend* (relative values) predicted by EH for frequencies (force constants) in the H_3 , H_5 , H_7 , and H_9 series.

A detailed explanation of this intriguing finding is still being developed.

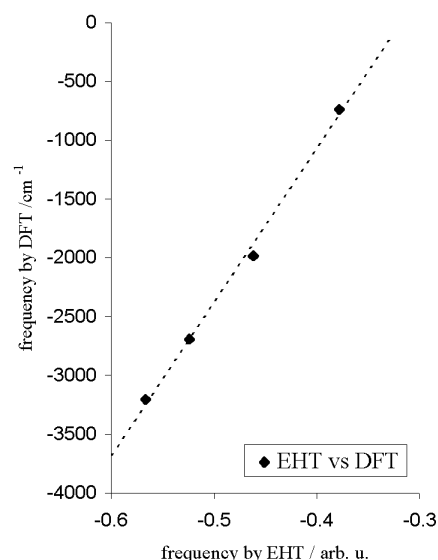


Figure 13. Correlation between the frequency of the imaginary mode for H_3 , H_5 , H_7 and H_9 computed by DFT (B3LYP/6-311++G**) and one computed by EH. Normal mode forms computed by DFT have been used for the EH calculation. Dotted line shows the linear regression with correlation coefficient of $R^2 = 0.996$.

- [3] We note here important contributions that introduce a model of superconductivity in real (and not reciprocal) space: a) K. H. Johnson, R. P. Messmer, *Synth. Met.* **1983**, *5*, 151–204; b) K. H. Johnson, M. E. McHenry, C. Counterman, A. Collins, M. M. Donovan, R. C. O’Handley, G. Kalonji, *Physica C* **1988**, *153–155*, 1165–1166; c) D. P. Clougherty, K. H. Johnson, M. E. McHenry, *Physica C* **1989**, *162–164*, 1475–1576. Nuclear dynamics is very important in the bipolaron model, as well: d) A. S. Alexandrov, P. P. Edwards, *Physica C* **2000**, *331*, 97–112. Important experimental indications have recently appeared on the dominant role of phonons for HTSC: e) A. Lanzara, P. V. Bogdanov, X. J. Zhou, S. A. Kellar, D. L. Feng, E. D. Lu, T. Yoshida, H. Eisaki, A. Fujimori, K. Kishio, J. I. Shimoyama, T. Noda, S. Uchida, Z. Hussain, Z. X. Shen, *Nature* **2001**, *412*, 510–514. In addition, BCS-type superconductivity in MgB_2 at temperature as high as 39 K has been recently reported: f) J. Nagamatsu, N. Nakagawa, T. Muranaka, Y. Zenitani, J. Akimitsu, *Nature* **2001**, *410*, 63–64. MgB_2 has held the record of the critical superconducting temperature among non-cuprate materials for a relatively short time (December 2000–August 2001); a hole-doped C_{60} with an expanded lattice is a new record holder with $T_C = 117$ K (J. H. Schön, Ch. Kloc, B. Batlogg, *Science* **2001**, *293*, 2432–2434).
- [4] Citation from: A. Simon, *Angew. Chem.* **1997**, *109*, 1872–1891; *Angew. Chem. Int. Ed. Engl.* **1997**, *36*, 1788–806.
- [5] Quite recently, a new M^{IV} -based ($M = Ti, Zr, Hf$) family of inorganic (here: not containing carbon) superconductors has been synthesized: a) S. Yamanaka, K. Hotehama, H. Kawaji, *Nature* **1998**, *392*, 580–582. Li_xHfNCl becomes superconducting at 25.5 K. Also, a new T_C record of 15.5 K for phosphide materials has been recently set by $MoRuP$: b) I. Shirota, M. Takaya, I. Kaneko, C. Sekine, T. Yagi, *Solid State Commun.* **2000**, *116*, 683–686. But it seems that *coincidence* rather than *rationale* or following up theoretical indications stood behind these discoveries, similar to the detection of superconductivity in fullerenes: c) A. F. Hebard, M. J. Rosseinsky, R. C. Haddon, D. W. Murphy, S. H. Glarum, T. T. M. Palstra, A. P. Ramirez, A. R. Kortan, *Nature* **1991**, *350*, 600–601, and in MgB_2 (Ref.[3f]).
- [6] Part 1: W. Grochala, R. Konecny, R. Hoffmann, *Chem. Phys.* **2001**, *265*, 153–163.
- [7] Part 2: W. Grochala, R. Hoffmann, *New J. Chem.* **2001**, *25*, 108–115.
- [8] Part 3: W. Grochala, R. Hoffmann, *J. Phys. Chem. A* **2000**, *104*, 9740–9749.
- [9] Part 4: W. Grochala, R. Hoffmann, *Pol. J. Chem.* **2001**, *75*, 1603–1659.

[1] J. Bardeen, L. N. Cooper, J. R. Schrieffer, *Phys. Rev.* **1957**, *108*, 1175–1204.

[2] J. G. Bednorz, K. A. Müller, *Z. Phys. B* **1986**, *64*, 189–193.

- [10] We have reported these findings at the 15th International Jahn–Teller Symposium “Vibronic Interactions in Crystals and Molecules” in Boston (USA), August 2000.
- [11] Note that $f_{AA} = 2 EN_A/R_{AB}$, is an equivalent of f_{AB} for the homonuclear triatomic AAA.
- [12] Gaussian94, Revision D.3, M. J. Frisch, G. W. Trucks, H. B. Schlegel, P. M. W. Gill, B. G. Johnson, M. A. Robb, J. R. Cheeseman, T. Keith, G. A. Petersson, J. A. Montgomery, K. Raghavachari, M. A. Al-Laham, V. G. Zakrzewski, J. V. Ortiz, J. B. Foresman, J. Cioslowski, B. B. Stefanov, A. Nanayakkara, M. Challacombe, C. Y. Peng, P. Y. Ayala, W. Chen, M. W. Wong, J. L. Andres, E. S. Replogle, R. Gomperts, R. L. Martin, D. J. Fox, J. S. Binkley, D. J. Defrees, J. Baker, J. P. Stewart, M. Head-Gordon, C. Gonzalez, J. A. Pople, Gaussian, Inc., Pittsburgh PA, 1995.
- [13] G. A. Landrum, “YAEHMOP: Yet Another extended Hückel Molecular Orbital Package.” A package for performing EH calculations on molecules and extended systems and visualizing the results, 1995. YAEHMOP is freely available for both Unix workstations and Power Macintosh systems on the WWW at <http://overlap.chem.cornell.edu:8080/yaehmop.html>.
- [14] C. A. C. A. O. (Computer Aided Composition of Atomic Orbitals), A Package of Programs for Molecular Orbital Analysis [PC Beta-Version 5.0, 1998], C. Mealli, D. M. Proserpio, A. Ienco, *J. Chem. Educ.* **1990**, 67, 399–402.
- [15] See selected references in the excellent review: T. Bally, W. T. Borden, Calculations on Open-Shell Molecules: A Beginner’s Guide. *Rev. Comput. Chem.* **1999**, 13, 1.
- [16] These are usually stretching, and not bending modes, which strongly influence transport of charge along such oligomer/polymer.
- [17] The H–H bond length of 0.931 Å has been fixed for all H–H separations, for all molecules investigated. This is the optimized bond length for a symmetric linear H₃ molecule.
- [18] To make graphical presentation easier, we adopt an arbitrary notation throughout the whole paper, making force constants for imaginary frequency modes negative. Typically one assumes that a force constant is positive and the corresponding frequency imaginary in such a case.
- [19] Using different terminology, it is a *second order Jahn–Teller effect*, or *pseudo Jahn–Teller effect*, which leads to instability of a linear symmetric H₃ molecule.
- [20] a) R. Peierls, *Ann. Phys. (Leipzig)* **1930**, 4, 121–148; b) R. E. Peierls, *Quantum Theory of Solids*, Oxford University Press, Oxford, 1955.
- [21] We adopt here the following notation for the H₃ molecule: σ_g is HOMO (= SOMO-1), σ_u is SOMO, and σ_g^* is LUMO (= SOMO + 1).
- [22] We could not compute the molar instability of the infinite H polymer by DFT due to symmetry breaking of the wavefunction for higher homologues in the [H_n] series. Obviously, global (and not molar) instability of [H_n] species strongly increases with *n*, leading to numerical problems in the calculations (very large forces acting at assumed molecular geometry), and to symmetry breaking of the wavefunction. This is why we only estimate the molar instability of the infinite H polymer using an extrapolation procedure.
- [23] The deformation of the 1D infinite chain described by us in this paper leads to charge density wave formation, if the vibrational quanta of the resulting (distorted) chain are neglected. But if the energy of the phonons of the distorted chain is large enough, the dynamic transformation between two equivalent potential energy minima is possible, possibly leading to superconductivity via a dynamic change in the lattice fluctuations. Thus, in our present paper, we have first tried to find preconditions for strong static deformation, and express them in a chemical language. We think that such attempts are valuable, considering the practical inability of existing physical models to design novel families of superconductors.
- [24] The linear symmetric geometry may not be the ground state geometry of the (A₃)^q species. For example, (H₃)⁺, (Li₃)⁺ and (F₃)⁺ prefer to be equilateral triangles, and (Li₃) is a nonequilateral triangle.
- [25] A detailed MO model to describe vibronic stability in the (H₃)^q series may be found in reference [9].
- [26] This choice corresponds to bond lengths optimized in the DFT calculation for uncharged radical species.
- [27] The frequency of the “pairing” phonon mode has been calculated by determining the square root of the total energy changes $(\Delta E_i)^{1/2}$ along the normal coordinate for this mode, $Q_i = Q_{opt}$ for a small movement of nuclei, $Q_i = 0.01$ Å. An infinite polymer built of equidistant H atoms with the H–H bond length of 0.931 Å has been assumed. A negative sign has been used for imaginary frequencies, for ease of graphical presentation. According to Hooke’s law for a harmonic oscillator, $E = \frac{1}{2}k(Q_i)^2$, and given $v = 2\pi^{-1}(k/m)^{1/2}$, one obtains that $v \sim (\Delta E_i)^{1/2}$. Thus, we have in fact calculated a parameter *linearly proportional* to vibrational frequency, *v*, and also proportional to force constant, *k* (consider that reduced masses for all normal modes of linear H_n molecules have the same value of 1 amu).
- [28] On general conditions for charge-density waves in different materials with partially filled bands see: a) M. H. Whangbo, E. Canadell, P. Foury, J. P. Pouget, *Science* **1991**, 252, 96–98; b) E. Canadell, M. H. Whangbo, *Chem. Rev.* **1991**, 91, 965–1034; c) M. H. Whangbo, *J. Chem. Phys.* **1981**, 75, 4983–4996.
- [29] k_u is zero for infinite A–B bond length. This indicates that the k_u versus A–B bond length function passes through a minimum for large A–B bond lengths. Thus, k_u is a monotonic and decreasing function of the A–B bond length only for A–B bond lengths close to the equilibrium value.
- [30] a) B. I. Swanson, M. A. Stroud, S. D. Conradson, M. H. Zietlow, *Solid State Commun.* **1988**, 65, 1405–1409; b) V. V. Shchennikov, *Phys. Status Solidi B* **2001**, 223, 561–565; c) D. Jaccard, H. Wilhelm, D. Jerome, J. Moser, C. Carcel, J. M. Fabre *J. Phys. Condens. Matter* **2001**, 13, L89–L95.
- [31] The “2s over 2p” region is, of course, unrealistic for F, as for any other element in the periodic table. Tuning of the orbital energy of 2s level of F so that it passes through the 2p level is, however, a good way in the EH theory for modeling the “avoided crossing” region.
- [32] One can also express s–p mixing through substantially increased polarizability (decreased hardness), or increasing contribution from excited states to the electronic wavefunction. Mixing of the electronic states and polarization in an electric field will be, of course, enhanced as the energy separation of the levels decreases. Alternatively, the concept of charge capacity might be used (charge capacity is the ability of an atom to absorb or yield electronic charge), since charge capacity may be related to the inverse of polarizability: P. Politzer, J. S. Murray, M. E. Grice, *Struct. Bond.* **1993**, 80, 102–114.
- [33] J. K. Burdett, *Inorg. Chem.* **1993**, 32, 3915–3922.
- [34] a) *The Metallic and Nonmetallic States of Matter* (Eds.: P. P. Edwards, C. N. R. Rao), Taylor and Francis, London, 1985; b) *Metal Insulator Transitions Revisited* (Eds.: P. P. Edwards, C. N. R. Rao), Taylor and Francis, London, 1995.
- [35] More precisely, when a Peierls distortion is small, metallic conductivity may be preserved. There is an interesting recent review on charge density wave and spin density wave superconductors: A. M. Gabovich, A. I. Voitenko, J. F. Annett, M. Ausloos, *Supercond. Sci. Technol.* **2001**, 14, R1–R27.
- [36] a) R. Reichlin, K. E. Brister, A. K. McMahan, M. Ross, S. Martin, Y. K. Vohra, A. L. Ruoff, *Phys. Rev. Lett.* **1989**, 62, 669–672; b) M. I. Eremets, E. A. Gregoryanz, V. V. Struzhkin, H. Mao, R. J. Hemley, N. Mudlars, N. M. Zimmerman, *Phys. Rev. Lett.* **2000**, 85, 2797–2800.
- [37] S. Desgreniers, Y. K. Vohra, A. L. Ruoff, *J. Phys. Chem.* **1990**, 94, 1117–1122.
- [38] A. San Miguel, H. Libotte, J. P. Gaspard, M. Gauthier, J. P. Itié, A. Polian, *Eur. Phys. J B* **2000**, 17, 227–233.
- [39] a) A. S. Balchan, H. G. Drickamer, *J. Chem. Phys.* **1961**, 34, 1948; b) B. M. Riggleman, H. G. Drickamer, *J. Chem. Phys.* **1963**, 38, 2721.
- [40] a) H. Luo, S. Desgreniers, Y. K. Vohra, A. L. Ruoff, *Phys. Rev. Lett.* **1991**, 67, 2998–3001; b) H. Luo, R. Green, A. L. Ruoff, *Phys. Rev. Lett.* **1993**, 71, 2943–2946.
- [41] M. I. Eremets, K. Shimizu, T. C. Kobayashi, K. Amaya, *Science* **1998**, 281, 1333–1335.
- [42] Iodide and hydride anions are often compared due to their similar properties (polarizability, redox behavior). Interestingly, CsH has not been metallized, in contrast to CsI: K. Ghandehari, H. Luo, A. L. Ruoff, S. S. Trail, F. J. DiSalvo, *Solid State Commun.* **1995**, 95, 385–388.
- [43] S. T. Weir, Y. K. Vohra, A. L. Ruoff, *Phys. Rev. B* **1987**, 35, 874–876.
- [44] a) C. Narayana, H. Luo, J. Orloff, A. L. Ruoff, *Nature* **1998**, 393, 46–49. Fluid H appears to be metallic at 140 GPa: b) S. T. Weir, A. C. Mitchell, W. J. Nellis, *Phys. Rev. Lett.* **1996**, 76, 1860–1863.

- [45] Frölich was the first to interpret (erroneously) the dielectric Peierls band gap as a superconducting one (H. Frölich, *Proc. Roy. Soc. A* **1954**, 223, 296–305).
- [46] V. V. Struzhkin, R. J. Hemley, H. K. Mao, Y. A. Timofeev, *Nature* **1997**, 390, 382–384.
- [47] K. Shimizu, K. Suhara M. Ikumo, M. I. Eremets, K. Amaya, *Nature* **1998**, 393, 767–769.
- [48] M. I. Eremets, V. V. Struzhkin, H. Mao, R. J. Hemley, *Science* **2001**, 293, 272–274.
- [49] K. Shimizu, N. Tamitani, N. Takeshita, M. Ishizuka, K. Amaya, S. Endo, *Phys. B* **1994**, 194, 1959–1960.
- [50] N. Takeshita, S. Kometani, K. Shimizu, K. Amaya, N. Hamaya, S. Endo, *J. Phys. Soc. Jpn.* **1996**, 65, 3400–3401.
- [51] Y. A. Timofeev, B. V. Vinogradov, V. B. Begoulev, *Phys. Solid State* **1997**, 39, 207–207.
- [52] a) E. N. Yakovlev, Y. A. Timofeev, B. V. Vinogradov, *JETP Lett.* **1979**, 29, 362–364; b) V. N. Bogomolov, *arXiv:cond-mat/0103099*, **2001**.
- [53] a) L. Gao, Y. Y. Xue, F. Chen, Q. Ziong, R. L. Meng, D. Ramirez, C. W. Chu, J. H. Eggert, H. K. Mao, *Phys. Rev. B* **1994**, 50, 4260–4263. In addition, superconductivity is often generated by doping in between the metallic and insulating regimes, b) P. P. Edwards, N. F. Mott, A. S. Alexandrov, *J. Supercond.* **1998**, 11, 151–154; c) A. R. Armstrong, P. P. Edwards, *Ann. Reports C* **1991**, 259–331.
- [54] a) An early observation was that “poor” metals, such as Hg or Nb, are superconducting, while “good” metals, such as Cu or Ag, are not; b) T. W. Barbee III, A. Garcia, M. L. Cohen, *Nature* **1989**, 340, 369–371; c) R. J. Hemley, *Science* **1998**, 281, 1296–1297.
- [55] M. T. Green, V. Robert, J. K. Burdett, *J. Phys. Chem. B* **1997**, 101, 10290–10294.
- [56] D. A. Goldhammer, *Dispersion und Absorption des Lichtes*, Leipzig, Teubner, **1913**.
- [57] K. F. Herzfeld., *Phys. Rev.* **1927**, 29, 701–705.
- [58] Interestingly, the same conclusions were reached by Batsanov (S. S. Batsanov, *Refractometry and Chemical Structure*, Van Nostrandt, Applied Science Library, New York, **1966**).
- [59] a) P. P. Edwards, M. J. Sienko, *Int. Rev. Phys. Chem.* **1983**, 3, 83–137; b) P. P. Edwards, M. J. Sienko, *J. Chem. Edu.* **1983**, 60, 691–696; c) D. E. Logan, P. P. Edwards in *The Metallic and Nonmetallic States of Matter*, Taylor and Francis, London and Philadelphia, **1985**, pp. 65–92; d) P. P. Edwards, R. L. Johnston, C. N. R. Rao, D. P. Tunstall, F. Hensel, *Phil. Trans. R. Soc. Lond. A* **1998**, 356, 5–22; e) P. P. Edwards, R. L. Johnston, F. Hensel, C. N. R. Rao, D. P. Tunstall, *Sol. State Phys.* **1999**, 52, 229–338.
- [60] Of course, different solid state materials, which crystallize in various crystal groups, usually have different Peierls distortion pathways. Also, a given solid may have several ways leading to an energetically comfortable packing of atoms, which manifest themselves as different polymorphs of a given substance.
- [61] R. G. Pearson, *Inorg. Chem.* **1988**, 27, 734–740.
- [62] J. B. Mann, T. L. Meek, L. C. Allen, *J. Am. Chem. Soc.* **2000**, 122, 2780–2783.
- [63] R. Hoffmann, *Solids and Surfaces*, VCH, Weinheim **1988**.
- [64] J. K. Burdett, *Chemical Bonding in Solids*, Oxford University Press, Oxford, **1995**.
- [65] A. W. Sleight, *Acc. Chem. Res.* **1995**, 28, 103–108.
- [66] a) W. Grochala, R. Hoffmann, *Angew. Chem. Int. Ed.* **2001**, 40, 2743–2781; b) W. Grochala, R. Hoffmann, *Angew. Chem.* **2001**, 113, 2816–2859.
- [67] Validity of the comparison presented in Figure 13 is assured by Hooke’s law (Ref. [27]).
- [68] **Note added in proof** (17.11.02): When this paper was in proof an important paper on superconductivity in pressurized lithium appeared: V. V. Struzhkin, M. I. Eremets, W. Gan, H.-K. Mao, R. J. Hemley, *Science* **2002**, 298, 1213–1215. Also, serious doubts arose about the validity of the experiments on charge-injected superconductors by Schon et al. (our ref. [3]).

Received: September 10, 2001
Revised: August 21, 2002 [F3546]